THE ASTROPHYSICAL JOURNAL, 408:230–238, 1993 May 1

η CARINAE: A NEW MODEL

J. M. BORGWALD
Department of Physics, Randolph-Macon College, Ashland, VA 23005

AND

M. W. FRIEDLANDER
McDonnell Center for the Space Sciences and Department of Physics, Campus Box 1105, Washington University, One Brookings Drive, St. Louis, MO 63130-4899

ABSTRACT

η Car is surrounded by a thick shell of dust whose infrared emission is close to $5 \times 10^6\ L_\odot$. We propose a new model for η Car, in which cosmic rays originate in a central object and stream out, losing energy in the gas and dust. This energy is subsequently radiated by the dust grains, with most of the energy coming from cosmic-ray protons having kinetic energies 1 MeV $< E <$ 10 MeV. Assuming for the cosmic-ray protons a differential kinetic energy spectrum of the form $E^{-2.5}$, the infrared spectrum can be very well fitted for wavelengths between 5 μm and 175 μm. The visual continuum exhibits features that strongly suggest the synchrotron mechanism. Tests of the model are provided through predicted fluxes of high- and low-energy gamma rays that will be produced through proton collisions in the gas and dust of the nebula.

Subject headings: circumstellar matter — cosmic rays — gamma rays: theory — infrared: stars — stars: individual (η Carinae)

1. INTRODUCTION

η Carinae is one of the most luminous objects in our Galaxy. Sometimes classified as a slow nova or supernova or as an irregular variable, it has no normal stellar image but rather displays at visual wavelengths a condensation several arcseconds in diameter, somewhat elongated in one direction, with some apparently related condensations a few arcseconds away. The central condensation has been termed the "homunculus" because of the appearance of limblike extensions. Speckle observations in the visible and near-infrared suggest the presence of some very small condensations within the central region, and early photographs from the *Hubble* telescope indicate the presence of jets.

By far the largest part of the present luminosity of 1.8×10^{40} ergs s^{-1} is at infrared wavelengths, but this was not recognized until the advent of the new generation of infrared detectors in the later 1960s. The present luminosity is very close to that deduced from its peak apparent visual magnitude of -1, observed in 1843. If the luminosity has been effectively constant over the intervening years, then the total energy radiated approaches 10^{50} ergs and is one of several indicators of η Car's unusual nature.

Between 1856 and 1866, the apparent visual magnitude changed from $\sim$0.5 to $\sim$7, and this has been interpreted as indicating the condensation of dust in a thick circumstellar shell. Over 90% of the radiated energy is now contained in the infrared, between 1.6 μm and 175 μm. There is general agreement that this strong infrared flux comes from a dust shell. Based on infrared observations, the mass of this shell has been estimated to be around 0.01–0.02 $M_\odot$. The dust region, now around 10″ across, is thought to envelop a central hot star, perhaps a supergiant of 100 $M_\odot$ or more, with a surface temperature of around 3×10^4 K (Davidson 1971). The predominantly short-wavelength radiation from such a star will be absorbed by the dust, which will then radiate in the infrared. Numerous authors have worked with models that differ mainly in their detail regarding the dust's spatial distribution and temperature gradient. These models require a dust mass of around 0.01–0.02 $M_\odot$ and temperatures of around 200 K in outer dust regions.

Although there appears to be a consensus on the general features of the central star/dust shell model described briefly above, there are several observations that do not fit easily, if at all. At high energies, X-rays have been observed by the *Einstein* satellite (*HEAO 2*). One of the regions of the high-energy gamma rays detected by the *COS B* satellite appears to be centered on or very close to η Car but the identification is not certain. The source of the energy for these high-energy photons is not readily seen in the usual model. Weak radio emission has been detected, but the inferred electron density is far from the values deduced from the intensities of visual emission lines (see § 3.1). Early results from the *Hubble Space Telescope* (Hester et al. 1991) reveal an elongated structure with jets at right angles to the lobes and show that η Car is even more complex an object than has been considered to date.

This therefore appears to be a suitable time to present a model that is very different from those considered until now and which has the merit of unifying a variety of observations while providing a good fit to the infrared spectrum that contains so large a fraction of the luminosity. From the proposed model, we are able to predict a flux of gamma rays. For gamma rays around 100 MeV, the predicted flux is somewhat lower than that observed from *COS B* but within the range accessible to the *Compton Observatory* (*GRO*); for gamma rays with energies in the range 1–10 MeV, no measurements have yet been reported.

In § 2, we give a general description of the observed continuum spectrum of η Car. In § 3, we describe the model that we have developed. The essential feature of this new model is that at the center of η Car there is a source of cosmic rays. The energy radiated by the dust (primarily in the infrared) is supplied by cosmic-ray protons which lose energy in traversing the gas and the dust grains. The heavily polarized visible continuum is interpreted as synchrotron radiation from cosmic-ray

electrons. The energy requirements for our model are shown to be consistent with those generally accepted in studies of the origin of cosmic rays.

In §§ 4 and 5, we explore two variants of the model and show that the infrared spectrum can be very well reproduced. In § 6 we show that the cosmic-ray model developed above can be used to predict a flux of high-energy gamma rays (above 100 MeV). In § 7, we calculate the flux of photons with energies in the range 1–10 MeV that would also be expected. In § 8, we discuss the visual continuum and show that it can be understood as synchrotron radiation from energetic electrons. The survival of dust grains against sputtering by cosmic-ray protons is discussed in § 9. Finally, in § 10, we discuss some of the problems that a comprehensive model must still deal with.

2. SPECTRUM AND LUMINOSITY

Estimation of the luminosity of η Car requires a knowledge of its distance and correction for interstellar extinction. There has been disagreement on both of these important points. Gehrz et al. (1973) obtained the value of 2.3 kpc, based on the observed angular expansion and on Doppler velocities measured by Thackeray (1961). Turner & Moffatt (1980) deduced a value of 2.7 kpc, based on a detailed examination of extinction for stars in the nearby clusters Tr 14, Tr 16, and Cr 228. McGregor, Hyland, & Hillier (1988) list the value 2.5 kpc. Where older distance estimates were as low as 1.5 kpc, most recent values seem to lie in the range 2.3–2.7 kpc. We adopt a value of 2.5 kpc but emphasize that our conclusions do not depend sensitively on the precise value for the distance.

To correct for interstellar reddening, we adopt the values $R = A_V/E_{B-V} = 3.0$ and $E_{B-V} = 0.4$. For the extinction corrections at visual wavelengths, we have used the tabulations of Savage & Mathis (1979). No corrections have been made for wavelengths longer than 1.6 μm. Because so much of the radiated energy lies in the infrared, our major conclusions are not sensitive to corrections at the shorter wavelengths. From the corrected flux values and for a distance of 2.5 kpc, and assuming isotropic emission, the total energy radiated by η Car in the various spectral regions has been calculated, and the results are listed in Table 1. All of the values listed in the table refer to emission from the dust shell, and no correction has been made for absorption within the shell.

At radio wavelengths, several early searches led only to upper limits being set to the possible flux. The only positive identification has come from Retallack (1981, 1983) who carried out a high-resolution (50″) scan of the Carina nebula at 1415 MHz and found η Car well resolved, with a flux value of 0.9 Jy. Jones (1973) located a 30 MHz source 14 minutes west of η Car, but the large beamwidth (about 0°.8) makes identification problematic.

Polarization at visual wavelengths was discovered by Thackeray (1956) and confirmed by Wesselink (1962), with polarization up to 40% being found in some places. Polarization was measured in white light, in blue light, and Hα, with no wavelength dependence being found. Polarization was observed in both continuum and high-velocity emission lines, but not in low-velocity lines.

Polarization measurements were also carried out by Visvanathan (1967) in the U, B, V, and R bands, and by Forbes (1971) in the J, H, K, and L bands. These observations did not resolve detail within η Car and showed overall polarizations of around 5% with essentially no wavelength dependence. Warren-Smith et al. (1979) used an electronographic polarimeter to map the polarization optically at 0″.7 intervals and have shown that the polarization pattern is very regular. The electric vectors follow almost circular contours, and the peak polarization is close to 40%.

There is a rich emission line spectrum at visual wavelengths that has been examined, for example, by Rodgers & Searle (1967) who reported a total line flux of 6.4×10^{-7} ergs cm^{-2} s^{-1} at Earth. This corresponds to a luminosity of 4×10^{38} ergs s^{-1}. This feature will not be discussed further; the energy it represents is much less than in the infrared continuum. Beneath the visual emission lines there is a continuum, measured most recently by Davidson et al. (1986).

TABLE 1

η CARINAE CONTINUUM

Spectral Region	Luminosity (ergs s^{-1})[a]
Infrared (1.6–175 μm)	1.8×10^{40}
UV visual and near-IR (1500 Å–2.2 μm)	2.6×10^{38}
X-rays (0.5–3.0 keV)	3.1×10^{33}
Gamma rays (~100 MeV)	2×10^{35}

[a] Calculated for 2.5 kpc.

3. A COSMIC-RAY MODEL FOR η CARINAE

Our model which will now be described is based on the assumption that, at the center, there is a compact source of cosmic-ray particles surrounded by the dust shell. We make no assumptions concerning the intrinsic nature of this central source, apart from its emission of cosmic rays. Cosmic-ray protons are assumed to lose energy in traversing the dust and gas and thus provide the energy which is radiated by the dust, predominantly in the infrared. Cosmic-ray electrons outside the dust produce the visible continuum that we interpret as synchrotron radiation. We assume spherical symmetry in our calculations.

Wickramasinghe (1971) and Spitzer (1978), among others, have considered the general problem of cosmic-ray heating of dust, but this has usually been within the context of interstellar situations where the flux of cosmic rays is too weak for them to produce heating to the temperatures observed in η Car. As will be shown, the heating of η Car's dust can be accomplished by cosmic-ray protons provided the central source is a significant but not unreasonably large contributor to the galactic cosmic-ray flux.

Cosmic rays will lose energy directly in both the gas and the dust, and the balance between these two components will depend on the gas density. In addition, there will be a transfer of energy (typically radiative) from gas to dust. Details of the model are sensitive to the gas density but there is considerable uncertainty regarding that density. Accordingly we first discuss the evidence that bears on this important item. Our model calculations have then been carried out for two representative values of the density: about 10^3 cm^{-3} (as suggested by radio observations of ionized gas) and 10^5 cm^{-3} (in closer conformity with the usual 100:1 gas:dust ratio).

3.1. *Gas in η Carinae*

Evidence for the gas density can be obtained from radio observations. There have been several radio surveys of the Carina nebula, the most recent having been carried out at 22 GHz by Tateyama, Strauss, & Kaufmann (1991), who have

presented a map with an angular resolution of 4'.3. There are strong similarities between their map and those of Shaver & Goss (1970) and Gardner et al. (1970), at 408 MHz and 5 GHz, respectively. In none of these maps does η Car appear as a recognizable feature.

The only radio observation that has thus far yielded a value rather than an upper limit for the flux from η Car is that of Retallack (1981, 1983), with the value of 0.9 Jy at 1415 MHz. Retallack (1983) has described the source as being "marginally resolved," with dimensions $40'' \times 20''$. Using the Schraml & Metzger (1969) expression relating flux density, source dimensions, and distance, we find $N_e = 940$ cm^{-3}. In this calculation, we have taken the temperature to be 10^4 K, and we assumed that N_e is constant throughout the radio-emitting region of effective diameter of $28''$ $(=40 \times 20)^{1/2}$. We then find a total gas mass of 0.48 $M_\odot$, of which only 0.0047 $M_\odot$ lies within the infrared emitting region. This latter gas mass is then comparable to the dust mass, and certainly far less than would be expected if the normal 100:1 ratio were applicable here.

This unusually low apparent gas mass is clearly a matter of concern. If even the central $6''$ (diameter) region actually contained ionized hydrogen at a temperature of 10^4 K and at a density of 4.8×10^5 cm^{-3} (about 100 times as much as the known density of dust), the 1415 MHz signal should amount to about 300 Jy, far larger than the observed flux.

Independent estimates of the electron density have been derived by Rodgers & Searle (1967) from the emission line spectrum. They have used a value of 1.5 kpc for the distance, and their results need to be adjusted to the greater distance now generally accepted. They employed values of $R = 6.0$ and $E_{B-V} = 0.69$ for their extinction corrections. We have not recomputed their emission line intensities, from which they have derived electron densities that are typically in the region of 10^5–10^6 cm^{-3} and emission volumes around 10^{49}–10^{50} cm^3. These are relatively small compared to the total volume of the dust shell, of 6×10^{51} cm^3. If we scale Rodgers & Searle's volumes to the 2.5 kpc distance we have used, we find volumes increased by a factor of 2.8 but still far smaller than the dust region.

Walborn & Blanco (1988) refer to an electron density of $10^{2.5}$ cm^{-3} based on earlier UV observations, and this is close to the value we have deduced from Retallack's radio measurement. On the other hand, Viotti et al. (1989), on the basis of *IUE* observations of line ratios, derive values in the range 10^6–10^{11} cm^{-3}.

Several authors have commented on the range of ionization energies indicated by the various emission lines observed. Some have raised the possibility of collision excitation, such as by an ionized wind from a star (Viotti et al. 1989). Some of the emission line observations suggest temperatures as high as 5×10^4 K. At this time, there seem to be no secure values for the gas and electron densities within and close to the dusty region. What is abundantly clear is the complex nature of η Car, both in its central condensation and the surrounding region.

We have therefore carried out calculations for a gas density of 10^3 cm^{-3} (close to what we have deduced from Retallack's observations) and for a representative higher value of 10^5 cm^{-3}. In the high-density case, the lowest energy protons do not penetrate completely through the gas and dust. For example, a proton of 1 MeV will penetrate less than 10^{16} cm or less than one-quarter of the distance through the dust. A proton requires an initial energy of at least 4 MeV in order to pass completely through all of the gas and dust. Accordingly, the low-energy end of the proton energy spectrum changes gradually with distance through the dust and the average energy loss in the gas and dust change in a nonlinear way. The energy lost by protons in traversing the gas is transferred promptly (by visible and ultraviolet radiation) to the dust grains and then radiated by the dust in the infrared. Much less particle energy is lost directly in the dust.

In contrast, in the low-density case, protons with energies of 1 MeV can penetrate the gas and dust shell and emerge with most of their initial energy. In this low-density case, the energy radiated by the dust derives in roughly equal parts from direct loss in the dust and from energy first lost in the gas. We will give separate discussions for the cases of high and low gas density, in §§ 4 and 5.

3.2. *General Description of the Model*

We assume that the dust shell extends from an inner radius R_1 from the central source to an outer radius R_2. At R_2, the flux of cosmic rays is J_2 particles cm^{-2} s^{-1}. Within this dust shell, we assume that the dust grains are distributed with a spherical symmetry and with a number density of $n = n_0 (R/R_2)^\alpha$/cm^3, where α is an adjustable parameter.

For the value of R_2, we used a value based on the infrared observations. Gehrz et al. (1973) reported a radius of $3''$ at a wavelength of 18 μm. Harvey, Hoffmann, & Campbell (1978) reported a "steep dust density gradient beyond the $6''$–$10''$ core," whereas Hackwell, Gehrz, & Grasdalen (1986) suggest an angular diameter about twice this size. Russell et al. (1987) have found nearly circular contours for their scans at wavelengths between 3.5 μm and 10 μm, with the diameter increasing from about $10''$ at the shorter wavelength to about $14''$ at 10 μm. We have carried out our calculations for both $3''$ and $6''$ angular radii, and the major conclusions are substantially insensitive to this choice. At a distance of 2.5 kpc, $3''$ corresponds to a distance of 1.13×10^{17} cm.

The radius of the inner boundary, R_1, is not well defined but it does relate to survival of the dust grains against proton collisions. In § 9 the effects of sputtering are considered, but in general the model calculations are not sensitive to the precise value provided that R_2 is much larger than R_1.

In our model, the cosmic rays are assumed to stream out radially. Energy will be lost by the cosmic rays directly in the dust grains and also in the gas from which it is radiated and promptly absorbed by the dust, to be subsequently reradiated by the dust (in the infrared). Throughout, we have assumed grain diameters $2a = 10^{-5}$ cm. Grain emissivities are assumed to depend on wavelength as $\epsilon = (2\pi a/\lambda)$, since most of the emitted radiation will be at wavelengths much greater than grain dimensions. This form of wavelength dependence for the emissivity is widely assumed (see, for example, Harvey et al. 1978), and it yields a Planck-averaged emissivity in good agreement with the calculations of Draine & Lee (1984) over the grain sizes and the range of temperatures that we expect to encounter with the grains in this region, i.e., 200–500 K. With this assumed form for the emissivity, it can be shown that the total emission from a single spherical grain of radius a can be simply described by $4\pi a^2 \sigma_1 T^5$ instead of the usual $4\pi a^2 \sigma T^4$, where we define $\sigma_1 = 16.74 a\sigma$ and σ is the Stefan-Boltzmann constant. For our calculations, we have divided the gas and dust region into concentric subshells each of thickness 10^{16} cm out to $R = 10^{17}$ cm, followed by an outer subshell of thickness 1.3×10^{16} cm.

At wavelengths greater than 1.5 μm, where the bulk of the dust emission lies, the optical depth is less than 0.25 and, for simplicity we ignore absorption of the infrared radiation in the dust. The total thermal emission from the dust is then evaluated as

$$L_{\rm IR} = \iint 4\pi R^2 n_0 (R/R_2)^{\alpha} 4\pi a^2 f(a, \epsilon, \lambda, T) dR\, d\lambda\ , \qquad (1)$$

where $f(a, \epsilon, \lambda, T)$ describes the thermal emission from each dust grain and T is the temperature of grains at radius R. Evaluation of n_0, T, and the cosmic-ray flux are described in the following sections. We note here that our best fits to the observations have come with $\alpha = 1$ and we confine ourselves to this value in further discussion. We have carried through parallel calculations for a constant dust density, that is, for $\alpha = 0$, and the result is a fit that is nearly as good. The value $\alpha = 1$ corresponds to a grain number density that increases with distance; a similar conclusion was reached by Andriesse (1976).

Our model has been built on the assumption that the heating of the dust comes from energy lost by cosmic rays. We have implicitly ignored any contribution from a hot central object. We would here argue that the luminosity of any central object must be much less than the present (infrared) luminosity of the dust. We have made some calculations for a model with a central 30,000 K source of the required luminosity, and for grain radii of 3×10^{-5} cm and 5×10^{-6} cm. In these models, we have assumed exponential absorption by the dust with no scattering. We have adjusted the overall amount of dust to yield a total optical thickness (in the visual and UV) of between 3 and 5 so that enough energy survives from the central source to provide the observed visual luminosity. In these models, we were unable to match the observed infrared spectrum; in all cases, the calculated spectrum was too weak at wavelengths longer than 20 μm and far too strong at shorter wavelengths because the inner part of the dust shell was very warm. The spectra peaked between 5 and 15 μm instead of the observed 20 μm. We also note that if the optical depth were only 3–5, there would be insufficient dust to radiate the observed infrared energy. We have concluded that we were unable to obtain a satisfactory fit with any of these models.

All of this still leaves unanswered the question of the nature of whatever there is at the center of η Car's dust shell. Without wishing to press the comparison too far, we note that the Crab's central pulsar has a luminosity in electromagnetic radiation far less than that which emerges from its surrounding nebula. There is no observational evidence for the presence of a pulsar within η Car, but we are unaware of any such radio search being conducted for η Car. With all of these considerations, we have therefore confined our further attention to our model of cosmic-ray heating.

4. HIGH GAS DENSITY CASE

4.1. *General Features*

With the high-density gas ($N = 10^5$ cm^{-3}), it is necessary to track the changing flux and energy spectrum of the protons with distance through the dust in order to calculate the energy loss within each subshell and thence the grain temperature. We also need to assume a shape for the proton differential kinetic energy spectrum and we adopt the form $dJ = KE^{-2.5}dE$ protons cm^{-2} s^{-1} MeV. The value 2.5 assumed for the energy power-law exponent was chosen to be similar to the value widely observed for cosmic rays near the Earth, though generally at higher energies where the modulating effects of the solar wind are small. The true shape of the primary cosmic-ray spectrum is not known at the low energies we need. Most of the energy loss comes from the lowest energy protons, those in the range 1–10 MeV. Protons with energies below 1 MeV will penetrate only a very short distance and we do not consider them further.

For the rate of loss of energy by the protons in the gas, we have parameterized the range-energy data listed by Trower (1966) for energy loss in hydrogen, to derive the expression $dE/dR = 677E^{-0.81}$ MeV/(g cm^{-2}).

The required cosmic-ray flux can then be calculated by considering the energy loss in each subshell and equating the total to the emitted IR energy, assuming that all of the energy lost in the gas is promptly transferred to the dust, a reasonable assumption given the large visible and ultraviolet optical thickness in the dust. From these calculations, we find the flux of protons at the inner dust boundary to be $2.5 \times 10^{11}E^{-2.5}$ protons cm^{-2} s^{-1} MeV, for $E > 1$ MeV.

With this value, we find the grain density at the outer boundary to be $n_0 = 7.3 \times 10^{-6}$ cm^{-3}. The total dust mass is then 4×10^{31} g or 0.02 $M_\odot$. In this calculation, the temperature of the grains was found to range from 325 K at $R_1 = 6 \times 10^{16}$ cm to 150 K at $R_2 = 1.13 \times 10^{17}$ cm.

4.2. *Cosmic-Ray Energetics*

With a differential energy flux of $2.5 \times 10^{11}E^{-2.5}$ protons cm^{-2} s^{-1} MeV entering the dust region at $R_1 = 6 \times 10^{16}$ cm, the cosmic-ray luminosity (total kinetic energy carried by the protons) is 3.7×10^{40} ergs s^{-1}. Half of this is lost in the gas and dust and then radiated, and the remainder is carried by protons that emerge from the dust shell.

The value for the cosmic-ray luminosity that we have calculated above can be compared with a value obtained from general cosmic-ray considerations. Based on near-Earth observations, the average cosmic-ray energy density in the galaxy is around 1 eV cm^{-3}. The average cosmic-ray lifetime, based on the abundance of the secondary product ^{10}Be, is around 10^7 yr, and an average cosmic-ray input of around 5×10^{40} ergs s^{-1} is generally considered to be needed to preserve a steady state (Gaisser 1990).

It is not unreasonable to consider a source whose current cosmic-ray luminosity is comparable to the probable average steady-state input power required for the galactic cosmic rays. The origin of cosmic rays is far from being well established. It is thought that active stellar objects such as supernovae or Wolf-Rayet stars are probably responsible, but it is not yet clear where the cosmic-ray acceleration occurs, either directly or by expanding shocks from these active stars.

If η Car is truly a source of cosmic-ray protons with the assumed energy spectrum and with the fluxes we have calculated, then we would expect to observe other secondary effects, and these are addressed in §§ 6 and 7.

4.3. *The Infrared Spectrum*

The preceding calculations have made use only of the total thermal energy emitted from the η Car dust grains. We can now use our model to calculate the spectrum of that thermal emission.

In our calculation, we have considered a sequence of concentric subshells between R_1 and R_2. The ingredients in this calculation are the numbers already determined: the cosmic-ray

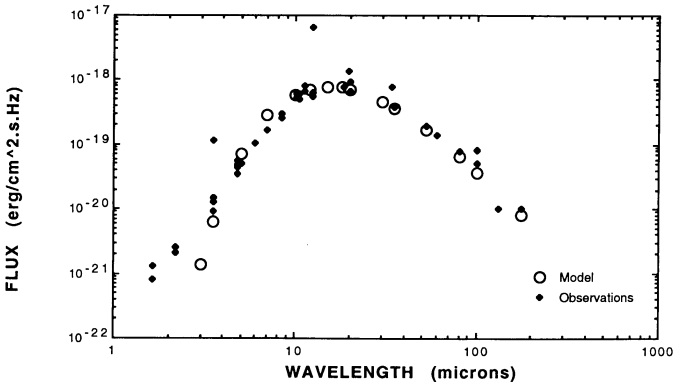

FIG. 1.—Infrared spectrum from the dust shell for the high-density case. Observed flux values are indicated by filled squares; calculated fluxes from our model are indicated by open circles.

flux, the thickness of each subshell, the shape of the cosmic-ray energy spectrum, and the emissivity of the grains. We also need and have computed the average proton energy loss in the gas to be about 10^{-23} ergs cm^{-1}, falling slowly with distance from R_1 to R_2. Normalization is provided by the observed IR luminosity. The parameters still to be evaluated are the temperatures and numbers of the dust grains. We obtained our best fit to the IR spectrum with $T = 150$ K in the outermost subshell and with $n = 7.3 \times 10^{-6}(R/R_2)^{\alpha}$ cm^{-3}, and with $\alpha = 1$.

The resulting spectrum for the case of high gas density is displayed in Figure 1, along with the observed data points. The agreement between our model calculations and the observations is excellent for wavelengths longer than about 5 μm. From the peak of the spectrum and out to the longest wavelengths, the spectrum has comparable contributions from all of the subshells, but emission from the fewer but warmer inner grains dominate at the shorter wavelengths.

At wavelengths of 3 μm and less, our calculated spectrum falls increasingly below the observed values. In § 8, we suggest that another mechanism contributes at these shorter wavelengths.

5. LOW GAS DENSITY

5.1. *Energetics*

In this case, the energy lost directly in the dust grains becomes important, but first we must evaluate the dust grain number density. Earlier, we had given in equation (1) an expression for the total thermal emission from the dust grains. If the protons stream directly out, then the energy deposited in each grain will decrease as $1/R^2$. With the assumed form for emissivity, the total emission from each grain varies as T^5. Accordingly, the grain temperature at distance R from the center will scale as $T_2(R_2/R)^{2/5}$, where T_2 is the temperature at the outer boundary. The expression for L_{IR} then becomes

$$L_{IR} = 0.151 a^3 T_2^5 n_0 R_2^{2-\alpha} \int R^{\alpha} dR$$

$$= 1.8 \times 10^{40} \text{ ergs s}^{-1} \text{ observed} . \quad (2)$$

Determination of n_0 depends on T_2 and R_1. For this low-density case, we use $T_2 = 200$ K and $R_1 = 6 \times 10^{16}$ cm and discuss the reason for the choice of these values in § 5.2. We find $n_0 = 5.8 \times 10^{-6}$ cm^{-3} and the total mass of dust to be 3.2×10^{31} g or $0.016\ M_{\odot}$.

The cosmic-ray energy loss mechanism in the dust grains is described by the Bethe-Bloch relation but this must be used with some caution. A fraction of the energy lost by the cosmic rays goes to electrons that receive energies of several keV and promptly escape from the grains into the surrounding gas. Energy lost very close to a cosmic-ray path in a dense medium is sometimes termed the "restricted energy loss," and this has been separately tabulated for example by Atkinson & Willis (1957) and Ritson (1961).

For silicate grains, the restricted energy loss for protons in the low-energy region of interest here, can be well represented by

$$-dE/dx = 7.54 \times 10^{-4}/E^{0.84} \text{ ergs cm}^{-1} , \quad (3)$$

where the proton energy E is in MeV. With our assumed energy spectrum, the average energy loss of a proton in a grain of diameter 10^{-5} cm is 3.2×10^{-9} ergs. We can calculate the total number of cosmic-ray grain traversals per second by combining this value with the known luminosity. We then find that the number of grain traversals per second is 5.5×10^{48} s^{-1}.

The total number of grain traversals per second is also given, in terms of the proton flux and the number and size of grains, by

$$4\pi^2 J_2 a^2 n_0 R_2^{2-\alpha} \int R^{\alpha} dR . \quad (4)$$

With the values for n_0 determined above, we obtain $J_2 = 1.9 \times 10^{12}$ protons cm^{-2} s^{-1}. We then derive a total proton flux of 3×10^{47} protons s^{-1} through the dust shell. With the assumed energy spectrum, the average proton energy is 3 MeV, so that the cosmic-ray luminosity of the presumed source is $L_{CR} = 1.4 \times 10^{42}$ ergs s^{-1}. For R_1 no larger than about 6×10^{16} cm, these values of the flux and luminosity are not sensitive to the precise value of R_1. For the alternative 6″ radius, the value of J_2 is unchanged but $L_{CR} = 6 \times 10^{42}$ ergs s^{-1}. These values are very much greater than L_{IR}, implying that most of the cosmic-ray energy is carried beyond the dust shell. No observed features have yet been identified with this amount of emerging energy, but we note that there have been observations of outlying condensations of η Car that suggest an outflow velocity of 800 km s^{-1} (Meaburn, Wolstencroft, & Walsh 1987).

These values of L_{CR} are also much larger than we found in the high-density case and uncomfortably larger than those usually considered acceptable for cosmic-ray sources. It is not impossible that an occasional cosmic-ray source should have such a large luminosity, but it is still a cause for concern.

Thus far, in arriving at these estimates of L_{CR}, we have considered only the energy lost directly in the dust grains. With a gas density of around 10^3 cm^{-3}, there will be a comparable amount of energy lost in the gas and promptly transferred to the dust grains. The result of including the energy transferred to the dust via the gas is to halve the required L_{CR} values but this still leaves them uncomfortably high, around 10^{42} ergs s^{-1}.

We have also briefly examined a different cosmic-ray heating model, in which the cosmic rays are assumed to diffuse rather than stream radially out. In this case, with constant diffusivity and no sources of particles within the dust, the flux of cosmic rays through the dust decreases as $1/R$. The net effect is to

increase the relative cosmic-ray heating of the outer regions and to reduce the required cosmic-ray flux.

5.2. *The IR Spectrum*

The best fit to the IR spectrum in this low-density case is obtained with $\alpha = 1$ and $T_2 = 200$ K, with $n_0 = 5.8 \times 10^{-6}$ cm^{-3} for the grain number density at the outer boundary, R_2. For a 6″ radius, the corresponding values are $n_0 = 5.1 \times 10^{-7}$ cm^{-3} and $M_{\rm dust} = 3.2 \times 10^{31}$ g. The outer temperature of 200 K is set mostly by the long-wavelength measurements of Harvey et al. (1978) and Ghosh et al. (1988). In the low-density case, this outer temperature cannot be changed by more than about 10% without significantly diminishing the goodness of fit to the IR spectrum, but a comparably good fit can be obtained with $R_1 = 5 \times 10^{16}$ cm and the corresponding value for n_0. Smaller values of R_1 have been examined, but these add little since the added volumes are small and the assumed grain number densities also decrease.

Computation of the IR spectrum proceeds as before, by evaluating the emission from each subshell. The grain temperatures in this low-density case are found to range from 250 K at the inner boundary to 200 K at the outer edge. The computed IR spectrum, displayed in Figure 2, is comparable to that obtained in the high-density case.

6. HIGH-ENERGY (>100 MeV) GAMMA RAYS

There has not yet been any definitive observation of gamma rays from η Car. However, there has been a possible detection by the satellite *COS B* which had an angular resolution of about 0°.5. Swanenberg et al. (1981) have published a list of 25 high-energy ($E \geq 100$ MeV) gamma-ray sources detected by *COS B* satellite. Only four of these sources were identified with known objects. Two adjacent sources were listed as 2CHG 284−00 and 288−00 with the comment "could be an extended feature." However, one of these, 2CHG 288−00 is close to η Car (288, −0.6), and examination of the profiles given by Hermsen (1980) supports our contention that 2CHG 288−00 can be identified with η Car. The profiles show that 2CHG 288−00 is concentrated around the position of η Car.

Montmerle (1981) and Issa & Wolfendale (1981) have suggested that 2CG 288−00 could be identified with the extended Carina nebula rather than with η Car, and they have proposed models in which the gamma rays come from the decay of neutral pions produced by cosmic-ray collisions in the extended region. Reanalyses of the *COS B* observations (Mayer-Hasselwander & Simpson 1989; Mayer-Hasselwander 1990) have reached the same conclusion.

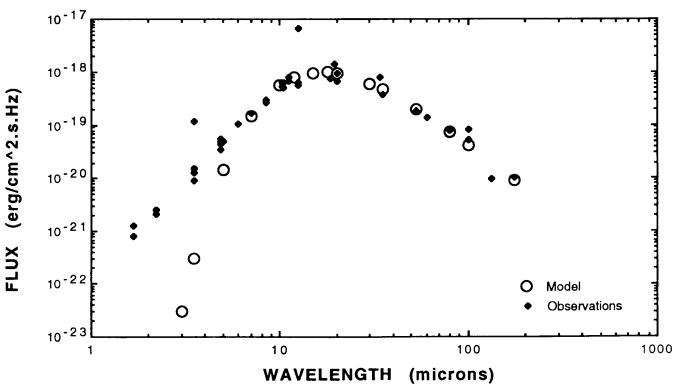

FIG. 2.—Infrared spectrum from the dust shell, for the low-density case. Observed flux values are indicated by filled squares; calculated fluxes from our model are indicated by open circles.

However, there is an alternative explanation, viz. that η Car and not the extended nebula is the source of the high-energy photons, still through neutral pions. This possible interpretation cannot be ruled out by the present limited observations (Hermsen 1991). The angular resolution of *COS B* does not permit a clear choice to be made. As will be shown below, a direct extrapolation of the cosmic-ray spectrum we have used in the dust model leads to a predicted photon flux not too far from the observed *COS B* value.

If the energy spectrum of the cosmic-ray protons extends up to the GeV region, then we would expect collisions with the surrounding dust to produce neutral pions. Production of the pions can be described in the following way:

$$dN/dt = 2[J_2(R_2/R)^2][4\pi R^2\, dR][n_n(R/R_2)^\alpha]\sigma \text{ photons s}^{-1}, \quad (5)$$

where dN photons come from pions produced in a spherical shell of thickness dR at radius R from η Car. The cross section for neutral pion production is σ. The initial factor of 2 represents the number of photons per pion. We assume that the cross section is the same for collisions with protons and neutrons making up the grains. Values for the number of nucleons, R_2 and J_2 come with no adjustment from our earlier dust calculations and the assumed density of the gas. The third term in brackets ($n_n[R/R_2]$) describes the number of nucleons cm^{-3}.

Values for σ come from Stecker (1973):

$$\sigma = 2.1 \times 10^{-28}\, E^{0.53} \text{ cm}^2 \quad (\text{for } E > 700 \text{ MeV}), \quad (6a)$$

$$\sigma = 1.20 \times 10^{-48}\, E^{7.64} \text{ cm}^2 \quad (\text{for } 400 < E < 700 \text{ MeV}). \quad (6b)$$

(In these, E is in MeV.)

The energy spectrum of the photons will have a wide distribution peaking around 100 MeV and with a slope at high energies similar to that of the protons. Stephens & Bhadwar (1981) have undertaken detailed calculations for pion production and have shown that only about 50% of the resulting photons will have energies in the region 100–400 MeV, the range accepted in the *COS B* survey.

For the high-density case, we then find that the flux of high-energy photons at Earth from the inner 6″ diameter gas as N_γ (100—400 MeV) $= 3.6 \times 10^{-8}$ cm^{-2} s^{-1}, from the dust 1.6×10^{-8} cm^{-2} s^{-1} and from the radio halo 1.2×10^{-7} cm^{-2} s^{-1}, making a total of 1.7×10^{-7} cm^{-2} s^{-1}.

For the low gas density case, we obtain for the flux of photons at Earth, produced by collisions in the dust N_γ (100–400 MeV) $= 5 \times 10^{-8}$ cm^{-2} s^{-1}, with about 1.5×10^{-8} cm^{-2} s^{-1} from the gas occupying the same volume and 1.4×10^{-7} cm^{-2} s^{-1} from the radio halo (28″ diameter), yielding a total of 2×10^{-7} cm^{-2} s^{-1}.

These calculated values can be compared to the flux of 1.6×10^{-6} photons cm^{-2} s^{-1} observed by *COS B* for the possible source 2CG 288−00. The difference between the calculated and observed fluxes is sensitive to the exponent of the proton energy spectrum. The calculated infrared spectrum is most sensitive to the proton energy spectrum between 1 MeV and 10 MeV but for the gamma-ray production we are making a large extrapolation. When extrapolating to proton energies above 400 MeV, where meson production begins, a change of

exponent from 2.5 to 2.4 increases the yield of 100 MeV photons by a factor nearly 2. Given the simplicity of the model, the agreement between the calculated and observed high-energy gamma ray fluxes is marginally satisfactory and neither rules out nor strongly supports our model. It does, though, suggest that careful observation of the η Car region would be worthwhile with the *Compton Observatory* (*GRO*), whose high-energy EGRET system has a sensitivity of 5×10^{-8} photons cm^{-2} s.

In our calculations above, we have assumed a simple spectrum in kinetic energy. We should note that some models of cosmic-ray origin and propagation have been phrased in terms of the particle momentum rather than energy. We have not carried out separate calculations using momentum, but note that momentum-based spectra will give results qualitatively similar to those based on kinetic (rather than total) energy and the projections for production of gamma rays will be little affected.

7. LOW-ENERGY GAMMA RAYS

Gamma rays of a few MeV will be produced by cosmic-ray collisions with many nuclei in the dust and gas. The composition of the dust has not been firmly established. Joyce (1975) and Russell et al. (1987) have reported observing an enhanced emission in the region of the well-known 10 μm silicate feature. We have therefore used the silicate composition listed by Seab & Shull (1983). This leads to a value of 2×10^7 oxygen atoms per grain.

Extensive data on cross sections have been tabulated by Ramaty, Kozlovsky, & Lingenfelter (1974). The calculation of the photon yield from collisions with oxygen in the dust grains is similar to that for the 100 MeV photons from neutral pions, but using the cross sections of Ramaty et al. covering proton energies between 10 and 200 MeV. The production cross sections lie in the range 15–150 mbarn for 6.1 MeV photons and 15–60 mbarn for 6.9 MeV photons.

For the high-density case, and with the same proton spectrum already used for the infrared calculations, we find the predicted flux of 6.1 MeV and 6.9 MeV photons at Earth is then calculated to be 2×10^{-7} photons cm^{-2} s^{-1} and 1×10^{-7} photons cm^{-2} s^{-1}, respectively. For the case of the low gas density, the flux of 6.1 MeV and 6.9 MeV photons at Earth is then calculated to be 3×10^{-6} and 1.5×10^{-6} cm^{-2} s^{-1} respectively.

These values approach the quoted sensitivity (3×10^{-6} cm^{-2} s^{-1}) for the COMPTEL system that is a part of the *Compton Observatory*. We do note, though, that in none of our calculations thus far have we allowed for the presence of cosmic rays heavier than protons. The typical cosmic-ray flux near the Earth has a helium component of the order of 10% of the abundance of the protons, at the same energy per nucleon. If the same relative abundance holds in η Car, then the helium-produced fluxes of low-energy gamma rays at Earth will be roughly equal to those from the proton collisions. This result comes from two factors: the helium cross sections between 2 and 10 MeV nucleon^{-1} are typically double those of the protons between 10 and 100 MeV, and the steep energy spectrum compensates for the lower intrinsic helium abundance.

If, instead of consisting of silicates, the grains are composed of graphite, we calculate that the flux of 4.4 MeV photons would be about 1×10^{-6} cm^{-2} s^{-1} in the high-density case and 7×10^{-5} cm^{-2} s^{-1} in the low-density case. Here again, these numbers refer to proton collisions; if there are helium nuclei with 10% of the abundance of the protons, then their collisions will yield an additional flux approximately equal to that from the proton collisions.

In summary, our calculations suggest that a search for 4 and 6 MeV photons would also be worthwhile.

8. OPTICAL CONTINUUM

Beneath the strong emission line spectrum at visual wavelengths, there is a continuum, described by Aller (1966) and by Rodgers & Searle (1967). More recently this has been measured by Davidson et al. (1986) who reported intensities at wavelengths of 1500 Å, 4700 Å, and 6900 Å. When we correct for interstellar absorption [using the data of Savage & Mathis (1979) with $E(B-V) = 0.4$], we find that these three most recent data points, together with the near-infrared intensities observed at 1.65 μm and 2.2 μm, can be very well represented by a simple power law in frequency, $I \sim \nu^{-\alpha}$, with $\alpha = (0.98 \pm 0.02)$ as shown in Figure 3. A power-law spectrum can result from synchrotron radiation produced by an ensemble of relativistic electrons with a power-law differential energy spectrum $n(E) \sim E^{-\gamma}$, where $\gamma = 2\alpha + 1$. For η Car's spectrum between 1500 Å and 2.2 μm, the electron energy spectrum thus appears to have an exponent $\gamma = 2.96 \pm 0.04$. This exponent is comparable to that of the primary cosmic-ray electron spectrum as observed near the Earth, and slightly steeper than the spectrum we have assumed for protons.

The addition of a synchrotron component compensates qualitatively for the rapid fall-off of the thermal spectrum from the dust in the near IR. In fact, at a wavelength of 3.5 μm, the sum of our suggested synchrotron component (3×10^{-21} ergs cm^{-2} s^{-1} Hz^{-1}) and our model's thermal emission (6×10^{-21} ergs cm^{-2} s^{-1} Hz^{-1}) amounts to about half of that observed (1.6×10^{-20} ergs cm^2 s^{-1} Hz^{-1}).

At shorter u–v wavelengths, Viotti et al. (1989) have reported measurements of the continuum between 1230 Å and 3175 Å. Their observed flux at 1516 Å agrees with the value obtained by Davidson et al. (1986) within about 10%, and their fluxes generally lie close to the $\nu^{-0.98}$ line that we derived (above). For example, at 1230 Å, our extrapolation predicts a flux of 5.3×10^{-23} ergs cm^{-2} s^{-1} Hz^{-1} as compared to the observed value of 5.8×10^{-23} ergs cm^{-2} s^{-1} Hz^{-1}. At the longer wavelengths, there is not as good agreement, with the observed values being higher than the fitted line by about a factor of 2, but *IUE* data cover a region of the spectrum where the extinction corrections are largest.

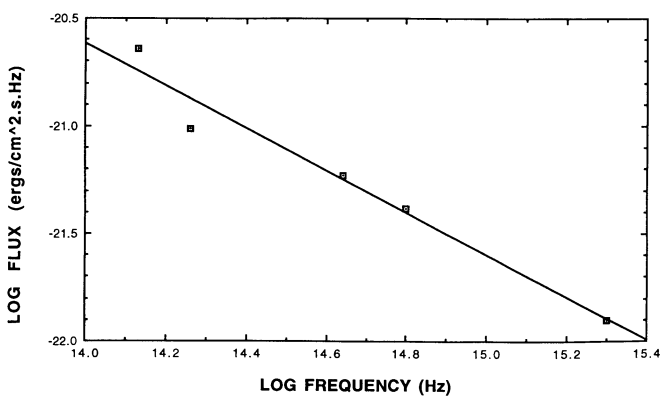

FIG. 3.—Observed continuum between wavelengths of 1500 Å and 2.2 μm. The line is a least-squares fit, showing a slope of $-(0.98 \pm 0.02)$.

The luminosity of η Car, represented by this continuum between 1500 Å and 2.2 μm, amounts to 2.6×10^{38} ergs s^{-1}. This is comparable to the luminosity of the Crab over a similar range of wavelengths, though the Crab spectrum is steeper ($\sim \nu^{-2.5}$) and the Crab's visual emission comes from a much larger volume.

Before the extent of the infrared spectrum was known, there had been suggestions that η Car might have a synchrotron spectrum (Searle, Rodgers, & Sergent [1965] and McCray [1967]) but there does not appear to have been any recent reappraisal. Two features of the visual continuum now suggest that this this mechanism be reexamined. The first feature is the shape of the continuum, as described above. The second is the polarization.

Warren-Smith et al. (1979) have mapped the linear polarization of η Car at intervals of 0".7, using a broad-band V filter. The polarization pattern that they found is remarkably similar to that observed at radio wavelengths for the Tycho supernova remnant (Duin & Strom 1975). For both objects, the electric vectors follow an almost circular pattern.

Pursuing our synchrotron model for the visual continuum, we will assume that the required relativistic electrons are moving in a region substantially outside the dust shell. There are two reasons for this choice. First, the visible nebula is larger than the infrared nebula. For example, the polarization mapping of Warren-Smith et al. extends out to a radius of about 8", compared to our assumed 3" radius for the dust shell. Second, although there will probably be relativistic electrons inside the dust shell, most of the visual radiation produced there will be strongly absorbed by the dust. We therefore assume that the radiating electrons are confined within a spherical shell of inner radius 3" and an outer radius of 8". The corresponding linear dimensions are 1.1×10^{17} cm and 3×10^{17} cm, with a contained volume of 1.1×10^{53} cm^3.

Synchrotron radiation emission depends on the electron number density, the field strength, and electron energy. For an electron energy of E MeV and a field of B gauss, the emission peaks around a frequency given by $\nu = 1.6 \times 10^7\ BE^2$ Hz (Webber, Simpson, & Cane 1980). We can derive values for the field strength and the total energy in electrons if we assume equipartition between the electron and field energies. We then find $B_{eq} = 3.2$ milligauss and $U_e = 4 \times 10^{46}$ ergs. With this value for B, our visual-to-near-IR continuum requires electrons with energies between 50 and 200 GeV, having corresponding half-lives between 4 and 20 yr. These energies are comparable to those required for the Crab's visual synchrotron emission, where the total energy is about 10^{48} ergs.

The polarization has generally been interpreted in terms of scattering of photons from the dust grains. Warren-Smith et al. (1979) developed a model in which the dust was concentrated in a toroidal circumstellar region, roughly at right angles to the line of sight. This can reproduce the polarization pattern, but does not explain the shape of the spectrum. We argue against the scattering model on several grounds.

First, from consideration of the infrared luminosity, there is general agreement that the dust mass lies in the range 0.01–0.02 $M_\odot$. For a grain diameter of 10^{-5} cm, the total optical thickness of the dust shell will then be in the range 20–30, the exact value depending on assumptions regarding the variation of grain number density with radial distance. With such a large optical thickness, virtually all of the radiation from any central star will be absorbed long before reaching the outer grains and none of the emerging optical photons should be original. Clumpiness of the dust could alter this conclusion but the required degree of clumpiness may be improbable, and it would appear surprising if this could be achieved and still maintain the degree of regularity seen in the pattern of the observed polarization.

Second, we note that no strong wavelength dependence has been observed. For example, Forbes (1971) observed polarizations using J, H, K, and L filters and observed polarizations of 2.1%, 4.6%, 2.4%, and 1.2%, respectively.

In summary, the shape of the continuous spectrum between 2.2 μm and 1500 Å and the polarization features are suggestive of a synchrotron source, but not conclusive.

9. SPUTTERING

Grains will be eroded through sputtering by the cosmic-ray protons. This effect has been studied generally at energies lower than concern us here. Dwek (1981) has discussed this process and given an expression for the sputtering yield (in atoms per collision) from silicates under thermal proton bombardment in a gas:

$$Y(E) = 0.03(0.160/E_{\mathrm{MeV}}) . \quad (7)$$

Other approaches to the sputtering process, such as that of Omaka & Kamijo (1978), suggest lower yields, and there is a paucity of experimental data for higher proton energies.

If we use Dwek's expression for $Y(E)$ and fold this with the proton flux and spectrum that we used for the infrared spectrum (conservatively using the larger flux appropriate to the low-density case), we calculate that a static grain at distance R cm from the center will have a half-life of $29(R/10^{16})^2$ yr. The lifetime of the grain is appreciably increased if we allow the grain to move out at a speed of 280 km s^{-1} (the average speed for the nebula to expand to 3" radius after 130 yr). For example, a grain will lose only 14% of its mass in the 34 yr that it takes to move from 10^{16} cm to 4×10^{16} cm. Given the uncertainty in the yield, Y, we take this calculation to indicate that the grains should survive for an adequate time, even though the proton flux is very high.

10. DISCUSSION

Our model represents a radical departure from the model that has been widely accepted until now, but it brings together a number of observations that the conventional approach has not connected. At this stage, it is not possible to set the values of several of the parameters with great precision. For example, the location of the inner boundary of the dust shell is poorly defined, but the total dust mass is largely insensitive to this. There is conflicting evidence bearing on the gas density. For both densities considered, the predicted flux of high-energy gamma rays is above the threshold of the *Compton Observatory*, and in the high-density case the cosmic-ray energetic requirements are reasonable. However, for both densities the predicted fluxes of low-energy gamma rays are close to the *Compton Observatory* threshold. For the low-density case the energy requirements are uncomfortably high.

We have not attempted to model the nonspherical shape of η Car, feeling that a simplified approach was adequate for this first attempt. Similarly, we have not considered the contribution to grain heating that could come from a hot central object in addition to the cosmic-ray protons.

As the cosmic rays lose energy, they will also eject some electrons which will themselves contribute to the heating of the

gas and some of this may reappear in the emission line spectrum, but we have made no attempt to examine this. There are additional features of η Car that do not yet find a place in our developing model. For example, there is a considerable record of the variability of the luminosity as well as much detail of the visual spectrum. See, for example, van Genderen & Thé (1984) for a survey of older literature and Zanella, Wolf, & Stahl (1984) for recent variability. The rich spectrum of emission lines has long been known, but several authors have commented on their inability to deduce consistent values for the electron density and temperature.

X-ray observations by the *Einstein Observatory* (Chlebowski et al. 1984) display a complex spectrum between 0.2 and 4 keV that has been interpreted in terms of an extended soft component and a central core with a hard spectrum. The integrated luminosity in the X-ray band is an order of magnitude less than that in the 100 MeV region (if our attribution of the *COS B* source 288 − 00 is correct). While the extended soft X-ray component has been explained in terms of an expanding shock, the central source has not yet found an explanation.

In summary, we consider that the cosmic-ray model merits further exploration, especially as more detailed observations become available from the *Hubble Telescope* and the *Compton Observatory*. The detection of 4 and 6 MeV gamma rays, and the confirmation of the 100 MeV observations of *COS B* would add great support to our model.

We are grateful to our colleagues in the McDonnell Center for the Space Sciences for various discussions as this model has been developed, and especially to Jonathan Katz for his many detailed and helpful comments on the manuscript. We are glad to acknowledge the helpful refereeing by R. D. Gehrz.

REFERENCES

Aller, L. H. 1966, Proc. Natl. Acad. Sci., 55, 671
Andriesse, C. D. 1976, A&A, 48, 137
Apruzese, J. P. 1975, ApJ, 196, 753
Atkinson, J. H., & Willis, B. H. 1957, UCRL Rep. 2426 Rev.; reprinted in Ritson (1961)
Chlebowski, T., Seward, F. D., Swank, J., & Szymkowiak, A. 1984, ApJ, 281, 665
Davidson, K. 1971, MNRAS, 154, 415
Davidson, K., Dufour, R. J., Walborn, N. R., & Gull, T. R. 1986, ApJ, 305, 867
Draine, B. T., & Lee, H. M. 1984, ApJ, 285, 89
Duin, R. M., & Strom, R. G. 1975, A&A, 39, 33
Dwek, E. 1981, ApJ, 247, 614
Forbes, F. F. 1971, ApJ, 165, L83
Gaisser, T. K. 1990, Cosmic Rays and Particle Physics (Cambridge: Cambridge Univ. Press)
Gardner, F. F., Milne, D. K., Mezger, P. G., & Wilson, T. L. 1970, A&A, 41, 349
Gehrz, R. D., Ney, E. P., Becklin, E. E., & Neugebauer, G. 1973, Astrophys. Lett., 13, 89
Ghosh, S. K., Iyengar, K. V. K., Rengarajan, T. N., Tandon, S. N., Verma, R. P., & Daniel, R. R. 1988, ApJ, 330, 928
Hackwell, J. A., Gehrz, R. D., & Grasdalen, G. L. 1986, ApJ, 311, 380
Harvey, P. M., Hoffmann, W. F., & Campbell, M. F. 1978, A&A, 70, 165
Hermsen, W. 1980, Ph.D. thesis, Univ. Leiden
———. 1991, private communication
Hester, J. J., Light, R. M., Westphal, J. A., Currie, D. G., Groth, E. J., Holtzmann, J. A., Lauer, T. R., & O'Neil, E. J. 1991, AJ, 102, 654
Issa, M. R., & Wolfendale, A. W. 1981, Nature, 292, 430
Jones, B. B. 1973, Australian J. Phys., 26, 545
Joyce, R. R. 1975, PASP, 87, 917
Martin, P. G. 1978, Cosmic Dust (Oxford: Clarendon)
Mayer-Hasselwander, H. A. 1990, private communication
Mayer-Hasselwander, H. A., Simpson, G. 1989, in EGRET Science Symp. (NASA CP 3071), ed. C. Fichtel, S. Hunter, P. Streekumar, & F. Stecker, 153
McCray, R. 1967, ApJ, 147, 544
McGregor, P. J., Hyland, A. R., & Hillier, D. J. 1988, ApJ, 324, 1071
Meaburn, J., Wolstencroft, R. D., & Walsh, J. R. 1987, A&A, 181, 333
Montmerle, T. 1981, Phil. Trans. R. Soc. Lond., A301, 505
Onaka, T., & Kamijo, F. 1978, A&A, 64, 53
Ramaty, R., Kozlovsky, B., & Lingenfelter, R. E. 1979, ApJS, 40, 487
Retallack, D. S. 1981, Proc. Astron. Soc. Australia, 3, 278
———. 1983, MNRAS, 204, 669
Ritson, D. M. 1961, Techniques of High Energy Physics (New York: Interscience), p. 196
Rodgers, A. W., & Searle, L. 1967, MNRAS, 135, 99
Russell, R. W., Lynch, D. K., Hackwell, J. A., Rudy, R. J., Rossano, G. S., & Castelaz, M. W. 1987, ApJ, 321, 937
Savage, B. D., & Mathis, J. S. 1979, ARA&A, 17, 73
Schraml, J., & Mezger, P. G. 1969, ApJ, 156, 269
Seab, C. G., & Shull, J. M. 1983, ApJ, 275, 652
Searle, L., Rodgers, A. W., & Sergent, W. L. W. 1965, Nature, 208, 1190
Shaver, P. A., & Goss, W. M. 1970, Australian J. Phys. 14, 77
Spitzer, L. 1978, Physical Processes in the Interstellar Medium (New York: Wiley-Interscience)
Stecker, F. W. 1973, ApJ, 185, 499
Stephens, S. A., & Badhwar, G. D. 1981, Ap&SS, 76, 213
Swanenberg, B. N., et al. 1981, ApJ, 243, L69
Tateyama, C. E., Strauss, F. M., & Kaufmann, P. 1991, MNRAS, 249, 716
Thackeray, A. D. 1956, Observatory, 76, 154
———. 1961, Observatory, 81, 99
Trower, W. P. 1966, High-Energy Particle Data Vol. 2, Lawrence Radiation Laboratory, UCRL-2426 (rev)
Turner, D. G., & Moffat, A. F. J. 1980, MNRAS, 192, 283
van Genderen, A. M., & Thé, P. S. 1984, Space Sci. Rev., 39, 317
Viotti, R., Rossi, L., Cassatella, A., Altamore, A., & Baratta, G. B. 1989, ApJS, 71, 983
Visvanathan, N. 1967, MNRAS, 135, 275
Walborn, N. R., & Blanco, B. M. 1988, PASP, 100, 797
Warren-Smith, R. F., Scarrott, S. M., Murdin, P., & Bingham, R. G., 1979, MNRAS, 187, 761
Webber, W. R., Simpson, G. A., & Cane, H. V. 1980, ApJ, 236, 448
Wesselink, A. J. 1962, MNRAS, 124, 501
Wickramasinghe, N. C. 1971, Nature Phys. Sci., 230, 166
Zanella, R., Wolf, B., & Stahl, O. 1984, A&A, 137, 79